Research Article

Ahmed A. H. Abdellatif*, Ahmed Abdelfattah, Mahmoud A. Younis*, Saed M. Aldalaan, and Hesham M. Tawfeek*

Chitosan-capped silver nanoparticles with potent and selective intrinsic activity against the breast cancer cells

https://doi.org/10.1515/ntrev-2022-0546 received August 11, 2022; accepted April 5, 2023

Abstract: Herein, we report on the development of chitosan-capped silver nanoparticles (AgNPs-CHI) with an intrinsic activity against breast cancer cells. Following chemical synthesis via a simple, one-pot reaction, the chitosan coating of AgNPs was verified using Fouriertransform infrared and ultraviolet-visible spectroscopies. The physicochemical properties and morphology were characterized using dynamic light scattering, scanning electron microscopy, and transmission electron microscopy. The shelf stability of the optimized platform was tracked for 3 months upon storage at either room temperature or 4°C. Then, the anticancer activities of AgNPs-CHI on human breast cancer cells, MCF-7, versus normal human cells, human skin fibroblasts (HSF), were evaluated via 3-(4,5-dimethylthiazol-2-yl)-2,5-diphenyltetrazolium bromide cytotoxicity assay and tumor-associated biomarkers determination by enzyme-linked immunosorbent assay, in comparison with plain silver nitrate (AgNO₃) solution. AgNPs were successfully coated with chitosan and demonstrated acceptable physicochemical properties, with a spherical morphology and high stability upon long-term storage. Although AgNPs-CHI and AgNO3 demonstrated

Graphical abstract

comparable cytotoxicity to MCF-7 cells, AgNPs-CHI resulted in 10-fold lower toxicity to HSF cells, suggesting a higher selectivity. In addition, AgNPs-CHI lowered IL-6 and tumor necrosis factor-alpha levels in MCF-7 cells by 90 and 30%, respectively, compared to 60 and 10% in the case of plain AgNO₃. The interesting therapeutic modality presented in this study is promising for potential clinical applications.

Keywords: breast cancer, silver nanoparticles, chitosan, IL-6, TNF- α

Industrial Pharmacy, Faculty of Pharmacy, Assiut University, Assiut 71526, Egypt, e-mail: heshamtawfeek@aun.edu.eg

Ahmed Abdelfattah: Department of Industrial Pharmacy, Faculty of

Pharmacy, Assiut University, Assiut 71526, Egypt

Saed M. Aldalaan: Department of Pharmacology, Faculty of
Medicine, Mutah University, Karak 61070, Jordan

1 Introduction

Cancer is a leading cause of death across the globe [1,2]. Breast cancer is still the most common and widely spread cancer in females. It has been recently estimated in 2020 that approximately 2.261 million new cases and 0.685 million deaths are related to this type of cancer globally [3]. It is also a multifunctional disorder with a high degree of inter-tumoral and intra-tumoral molecular and morphological heterogeneity [4]. The treatment strategy and clinical decision depend on the tumor subtype according to the estimated biomarkers and the pathophysiological and clinically collected data [5,6]. Non-selective or non-

HSPGs

HSPGs

AgNPs-CHI

AgNPs-CHI

Apoptosis

^{*} Corresponding author: Ahmed A. H. Abdellatif, Department of Pharmaceutics, College of Pharmacy, Qassim University, Qassim 51452, Saudi Arabia; Department of Pharmaceutics and Pharmaceutical Technology, Faculty of Pharmacy, Al-Azhar University, Assiut 71524, Egypt, e-mail: a.abdellatif@qu.edu.sa * Corresponding author: Mahmoud A. Younis, Department of Industrial Pharmacy, Faculty of Pharmacy, Assiut University, Assiut

Industrial Pharmacy, Faculty of Pharmacy, Assiut University, Assiut 71526, Egypt, e-mail: mahmoudyounis@aun.edu.eg

* Corresponding author: Hesham M. Tawfeek, Department of Industrial Pharmacy, Faculty of Pharmacy, Assiut University, Assiut

targeted therapy based on conventional chemotherapeutics is a two-edged weapon, considering its detrimental effects on healthy tissues. In addition, the tricky physicochemical properties of these agents, such as low aqueous solubility, poor diffusion into the tumor mass, and systemic toxicity, have collectively obliged scientists to develop new formulations to tackle these problems [7–9]. Different nanomaterials and their drug conjugates have shown promise and successful applications, especially in breast adenocarcinoma management [10,11]. Moreover, nanomedicines can act as a platform for the bioimaging of tumors [12].

Inorganic/metallic nanoparticles have attracted attention recently owing to their ease of fabrication, scalability, and interesting properties [13,14]. Silver nanoparticles (AgNPs) are considered the most relevant type of metallic nanomaterials in the area of anticancer therapeutics owing to their genotoxic effects and capability of programmed apoptosis induction [15,16]. In addition, it has been revealed that AgNPs can also modulate some interactions with the stromal cells and immune cells in the tumor microenvironment, which subsequently promote anticancer activity [17]. Increasing number of recent studies have demonstrated the high potential of AgNPs in the treatment of a wide variety of cancers including lung cancer, melanoma, hepatocellular carcinoma, glioma, prostate cancer, and multidrug-resistant tumors [18-20]. Moreover, it has also been demonstrated by other researchers that AgNPs have a potential role in the treatment of breast cancer [21-23]. Capping AgNPs with different polymeric materials can modulate their physicochemical properties, biodistribution, nanoparticles-cells interactions, cellular uptake, and intracellular silver ion release, which subsequently affect the selectivity, cytotoxic efficiency, and biosafety [24,25]. Pinzaru and coworkers reported on the increased stability and biotolerability of polyethylene glycol (PEG)-coated AgNPs [26]. A recent study performed in our group has shown the significant effect of AgNPs coated with ethyl cellulose on the inhibition of Tumor Necrosis Factor-alpha (TNF-α) in the breast cancer cell line, MCF-7 [27].

Chitosan (CHI) is a carbohydrate-based biopolymer that has been extensively investigated in the pharmaceutical literature as either a drug carrier or a coating material thanks to its ease of synthesis, economic price, biodegradability, and compatibility with most materials of pharmaceutical interest [28]. CHI has been investigated as a stabilizer and a functional coating for several metallic nanoparticles including platinum nanoparticles, gold nanoparticles, and copper nanoparticles [29,30].

In the present study, we investigated the impact of coating AgNPs with CHI on their performance against breast cancer cells. Our results revealed that chitosancapped AgNPs (AgNPs-CHI) demonstrated an interesting

potent and selective intrinsic anticancer activity against human breast adenocarcinoma cells, MCF-7, compared to a normal human cell model, human skin fibroblasts (HSF) cell line, as evidenced by a significant reduction in cell viability, Interleukin-6 (IL-6), and TNF- α levels. In contrast, plain silver nitrate solution (AgNO₃) showed significantly lower effects on the investigated tumor-associated biomarkers as well as non-selective cytotoxic effects, with severe damage to normal human cells. The therapeutic modality presented in this study holds promise as a non-classical treatment for breast cancer.

2 Materials and methods

2.1 Materials

Low molecular weight chitosan (50–190 kDa) and medium molecular weight chitosan (190–310 kDa) were purchased from Sigma Aldrich, USA. Human breast cancer cells (MCF-7) and HSF were obtained from American Type Culture Collection, USA, and were cultured and maintained according to the manufacturer's recommendations. 3-(4,5-dimethylthiazol-2-yl)-2,5-diphenyltetrazolium bromide (MTT) assay kit was purchased from Abcam, UK. Quantikine ELISA kits for human IL-6 and TNF- α were obtained from R&D Systems, USA. Bicinchoninic acid protein assay kit, radioimmunoprecipitation assay (RIPA) buffer, protease inhibitors, and phosphatase inhibitors were obtained from Thermofisher Scientific, USA. All the other used chemical reagents were of analytical grades and were used without further processing.

2.2 Preparation of AgNPs-CHI

Chitosan-coated AgNPs (AgNPs-CHI) were prepared according to the method reported by Mi *et al.* [31]. Fifty milligrams of CHI was dissolved in 10 mL of an aqueous solution of glacial acetic acid (10.0% v/v). Then, 5 mL of 1 mM AgNO₃ aqueous solution was added to the CHI solution, which was then diluted to 100 mL with distilled water. The solution was maintained in an ice bath with a constant stirring for 10 min. Reduction of AgNO₃ was mediated *via* the addition of 60 μ L of 0.1 M sodium borohydride (NaBH₄) dropwise while stirring for 45–60 min. Finally, the obtained AgNPs-CHI solution was kept at room temperature for another 15–30 min while being stirred. AgNPs-CHI dispersion was centrifuged, and then, the obtained pellets were dispersed in distilled water for being investigated in the subsequent experiments.

2.3 Characterization of AgNPs-CHI

2.3.1 Dynamic light scattering (DLS) studies

The geometrical particle size and the charge (ζ potential) of the produced AgNPs-CHI were determined by DLS using the Zetasizer Nano ZS analyzer (Malvern Instruments, UK) [32]. Simply, samples were adjusted to ~25°C and then exposed to a laser beam of ≈633 nm at a scattering angle of $\approx 90^{\circ}$. Samples were run 20 times, with a run time of 10 s. The average measurement of 3-6 formulations was considered and presented ± standard deviation.

2.3.2 Ultraviolet-visible (UV-Vis) spectroscopy

AgNPs-CHI solution was scanned from 300 to 600 nm using UV-VIS Spectrophotometer (Lambda 25, Perkin Elmer, Singapore). The absorbance spectra were plotted against the investigated wavelengths [33].

2.3.3 Fourier-transform infrared spectroscopy (FT-IR)

FT-IR spectrometer (Alpha II, model: Bruker, USA) was used to investigate the possible interaction and or coating of AgNPs with CHI. Spectra were collected from Solutions of medium molecular weight CHI, AgNO₃ (as a reference for silver), and AgNPs-CHI after their scanning from 4,000 to 400 cm⁻¹ as described previously [34].

2.3.4 Scanning electron microscopy (SEM)

The morphology and aggregation status of the optimized AgNPs-CHI were examined using an SEM microscope (Zeiss EVO LS10, Cambridge, UK), as described previously [35]. Samples were fitted to the stubs using a double-sided adhesive carbon tape and coated with gold under a vacuum in an atmosphere of the Argon gas for 120 s, prior to scanning and imaging using either a low magnification power or a high magnification power.

2.3.5 Transmission electron microscopy (TEM)

TEM was used to observe the morphology of the optimized AgNPs-CHI and estimate their particle diameter. Briefly, 10 µL of AgNPs-CHI solution was dropped onto the double-sided copper conductive tape surface and was allowed to dry overnight. Nanoparticles were visualized under the TEM microscope at 10–100k magnification power

using an accelerating voltage of 100 kV. (JEM-1230, JEOL, Japan) [36].

2.4 Physical stability assessment

The stability of the optimized AgNPs-CHI against aggregation was investigated after storage for 3 months at two different conditions: room temperature (\sim 25°C) and 4.0 \pm 0.5°C. The physical appearance of nanoparticles, including their color and morphology in addition to their particle size and zeta potential, were investigated at the beginning and the end of the storage period to judge their shelf stability.

2.5 Cytotoxicity study

The in vitro cytotoxicity of CHI, AgNPs-CHI, and AgNO₃ solutions was evaluated on MCF-7 cells versus HSF cells using MTT assay as reported previously [37]. Briefly, 3×10^{3} cells/well were seeded in 96-well plates 24 h prior to the experiments. Cells were treated with serial concentrations of the tested solutions in 50 µL of the corresponding growth medium. Forty-eight hours following the treatment, the media were aspirated, and the cells were incubated with 50 μL serum (-) medium and 50 μL of MTT reagent for 3 h at 37°C. Then, the cells were shaken with 150 µL of MTT solvent on an arbitrary shaker for 15 min. The absorbance of each sample was measured at 590 nm using BMG LABTECH®- FLUOstar Omega microplate reader (Allmendgrün, Ortenberg) and compared to the absorbance of non-treated cells after correction for the solvent background. The percentage of cell viability was plotted against the investigated concentrations, and the half-maximal inhibitory concentration (IC₅₀) values were calculated using Graphpad Prism 8 software.

2.6 Evaluation of tumor-associated biomarkers

The tumor-associated biomarkers, IL-6 and TNF-α, were assessed using an enzyme-linked immunosorbent assay (ELISA) as reported previously [32,38]. Sandwich ELISA protocol was adopted using pre-coated Quantikine® kits according to the manufacturer's recommendations. Cells were seeded as described earlier and treated with the investigated samples at concentrations corresponding to their IC₅₀ values for 48 h. Then, the cells were lysed using RIPA buffer supplemented with protease/phosphatase inhibitors, and the cell lysate was centrifuged at 15,000g, 4°C for

10 min followed by protein quantification via BCA assay. Samples were diluted with deionized water to obtain a working protein concentration of 1 mg/mL. Fifty microliters of the tested samples was then diluted with an equal volume of the specific assay diluent solution prior to their introduction into the pre-coated ELISA plates and incubated at room temperature for 2h. The plates were washed with wash buffer, treated with biotinylated antibodies, and incubated at room temperature for extra 2h followed by washing. A polymeric solution of horse radish peroxidase (HRP)-streptavidin was added to conjugate to the biotinylated antibodies and the color reaction is formed by the addition of tetramethylbenzidine (TMB) substrate solution. The color reaction was stopped with the kit's stop solution, and the absorbance was measured at 450 nm with correction by subtracting the readings at 540 or 570 nm. The biomarker concentration was calculated from a pre-constructed calibration curve and compared to the values of non-treated cells that were processed similarly.

2.7 Statistical analysis

Statistical analysis was performed using Graphpad Prism 8 software. One-way analysis of variance (ANOVA) followed by the Bonferroni test was used for multiple comparisons in a single cell line (one-factor experiments), while two-way ANOVA followed by the Bonferroni test was used for multiple comparisons in different cell lines (two-factor experiments). $P \le 0.05$ was considered to be statistically significant.

3 Results

3.1 Preparation and characterization of AgNPs-CHI

The efficiency of AgNPs-CHI synthesis was confirmed by the color change of the reaction medium to the characteristic yellow color 15 min following the addition of NaBH₄ solution.

To select the top-performing functional coating for AgNPs, CHI polymers with two different molecular weight ranges were investigated; namely low molecular weight CHI (50–190 kDa) and medium molecular weight CHI (190–310 kDa). The physicochemical properties of the resultant AgNPs were evaluated using DLS (Table 1 and Figure 1). The results revealed better physicochemical performance for the medium molecular weight CHI-coated AgNPs. Consequently, they were used for further experiments and referred to as chitosan-capped AgNPs (AgNPs-CHI) in the subsequent sections of this article (more details on the DLS images are shown Figures S1–S4).

The efficiency of the functional coating was characterized by UV-VIS and FT-IR spectroscopies. AgNPs-CHI demonstrated a single-band UV absorption spectrum with a maximum absorption wavelength (λ_{max}) of 405 nm (Figure 2). FT-IR spectra of plain AgNO₃, used as a reference, are shown in Figure 3a. Pure CHI demonstrated a broadband, with a peak at 3451.57 cm⁻¹, which refers to N–H and O–H stretching, and a characteristic double-spike peak at 1712.79 cm⁻¹ and 1636.89 cm⁻¹ for the NH₂ group (Figure 3b). AgNPs-CHI retained the reference peaks of silver, while the double-spike peak of CHI disappeared (Figure 3c).

The morphology of the optimized AgNPs-CHI was examined by SEM, where the micrographs revealed spherical nanoparticles, with uniform particle size and a minimal degree of aggregation (Figure 4). Moreover, TEM micrographs of AgNPs-CHI showed spherical nonaggregated particles with a metallic core having an average size of 20.88 ± 2.57 nm (Figure 5).

3.2 Physical stability assessment

AgNPs-CHI demonstrated high stability at the two investigated storage temperature conditions. They did not show any color change or precipitation during the 3-month evaluation period. Moreover, the physicochemical properties of AgNPs-CHI showed negligible changes after storage at either room temperature or 4°C, in comparison with the freshly-prepared counterparts (Table 2).

Table 1: Comparison of the physicochemical properties of AgNPs coated with chitosan polymers with two different molecular weight ranges (n = 6, average \pm standard deviation)*

	Hydrodynamic diameter (nm)	PDI	ζ Potential (mV)
Low molecular weight	623.66 ± 55.5	0.583 ± 0.09	8.67 ± 2.74
Medium molecular weight	287.43 ± 1.89	$\textbf{0.411} \pm \textbf{0.06}$	50.63 ± 2.2

^{*}The physicochemical properties were evaluated using DLS.

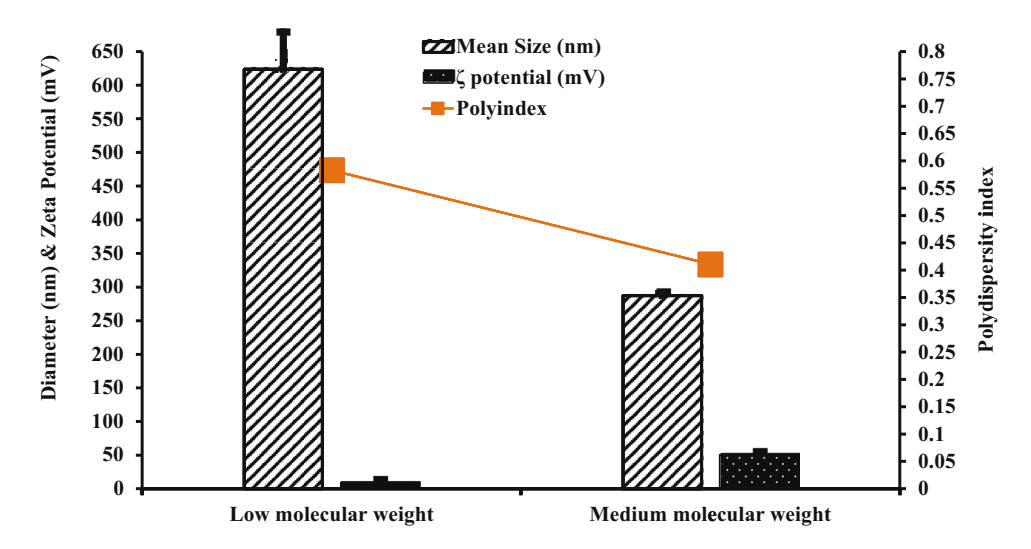


Figure 1: DLS of mean size (nm), zeta potential (mV), and polydispersity index of the formulated silver nanoparticles reduced with low and med molecular weight chitosan.

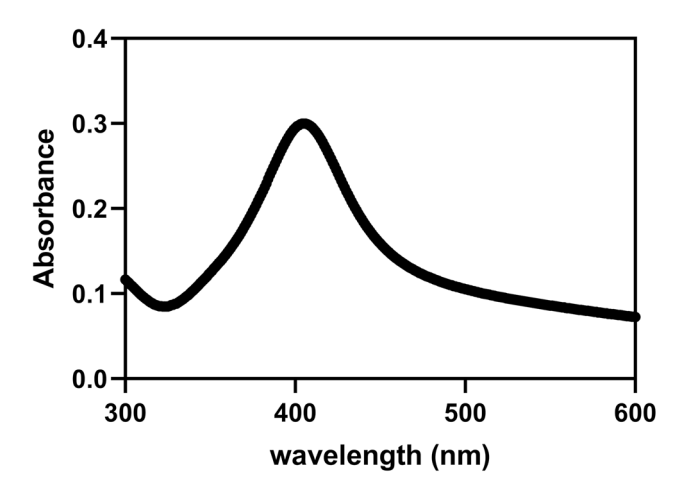


Figure 2: UV-Vis spectrum of the optimized AgNPs-CHI.

3.3 Evaluation of the anticancer activities of AgNPs-CHI

The anticancer performance of AgNPs-CHI was evaluated in MCF-7 cells (cancerous model) *versus* HSF cells (normal model) using cytotoxicity and ELISA assays. Interestingly, both AgNPs-CHI and plain AgNO $_3$ solutions demonstrated an intrinsic anticancer activity on MCF-7 cells with comparable cytotoxic effects, where the IC $_{50}$ values were 8.6 \pm 1.6 and 10.86 \pm 2.53 µg/mL for AgNPs-CHI and AgNO $_3$, respectively. Meanwhile, the CHI itself had a far lower toxicity with IC $_{50} \sim 100$ µg/mL. Surprisingly, AgNPs-CHI showed approximately 10-fold lower toxicity to HSF cells compared to AgNO $_3$ (IC $_{50}$ values were 29.63 \pm 4.32 and 3.35 \pm 0.5 µg/mL, respectively) (Figure 6a). Furthermore, AgNPs-CHI resulted in ~90% inhibition of IL-6 and

~30% inhibition of TNF- α in MCF-7 cells compared to only ~60% and ~10% inhibition of the same tumor markers in the case of AgNO $_3$ (Figure 6b and c).

4 Discussion

AgNPs are inorganic nanomedicines with a high potential for various therapeutic applications. Most previous studies investigated the application of AgNPs as drug carriers [39]. Nevertheless, the investigation of the intrinsic drug activities of AgNPs is still premature. Some previous reports discussed the potential cytotoxic activities of AgNPs which may be mediated via the induction of genotoxicity through interaction with the cellular DNA, and the subsequent induction of apoptosis [40]. Buttacavoli and co-workers reported on the maximum accumulation of Ag⁺ in the mitochondria and nuclei following the cellular uptake of AgNPs [41]. Yet, extending such property to the clinical level is still risky, taking into consideration the off-target toxicity that might be caused by the nonselective AgNPs. Our group has been investigating the functional coating of AgNPs aiming at modulating their efficiency and selectivity [27]. In the present study, we investigated the impact of coating with CHI on the intrinsic anticancer activity of AgNPs, applying breast cancer as a tumor model.

We investigated CHI with two different molecular weight ranges. Coating AgNPs with low molecular weight CHI resulted in nanoparticles with a larger particle size, a higher polydispersity, and a lower zeta potential, in

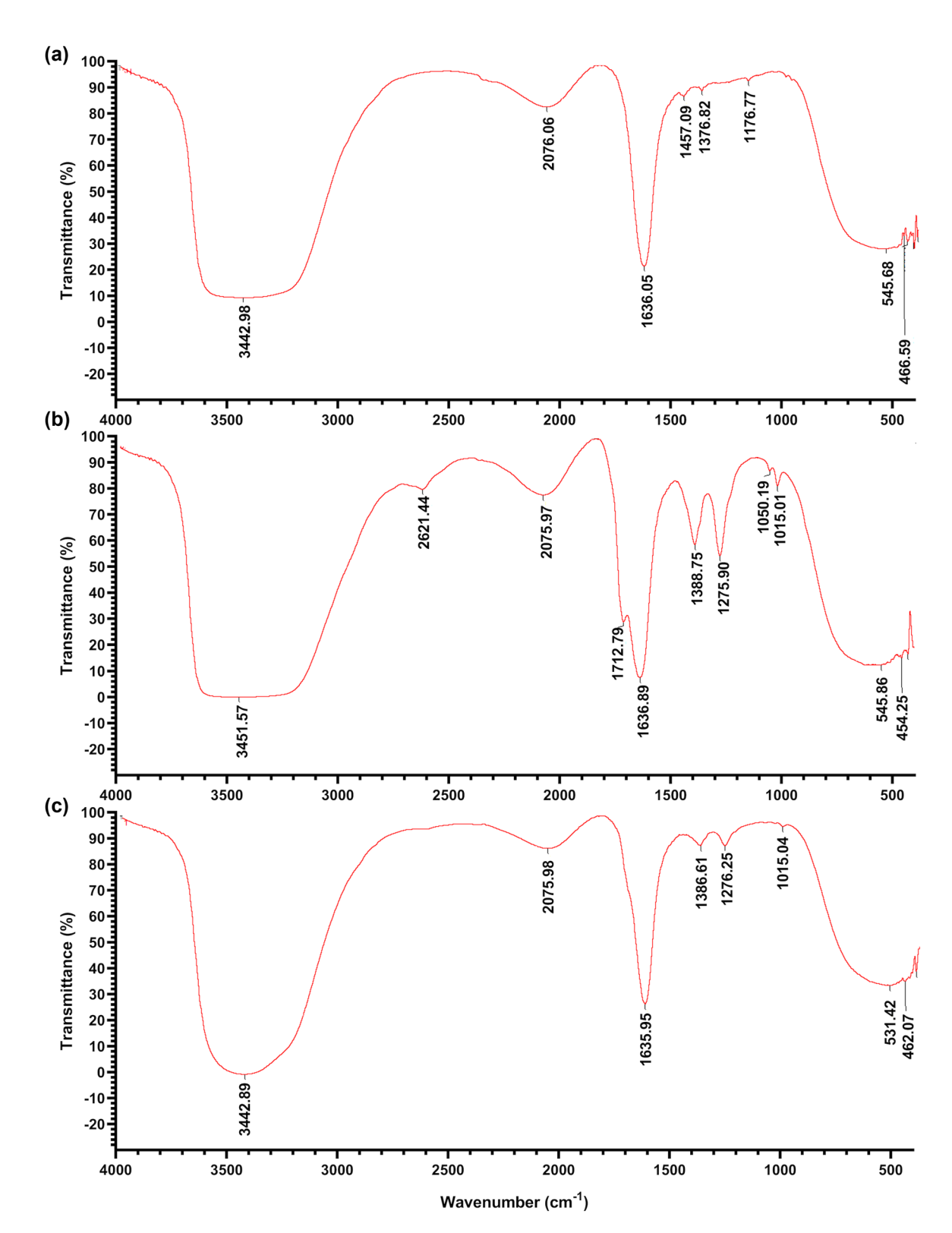
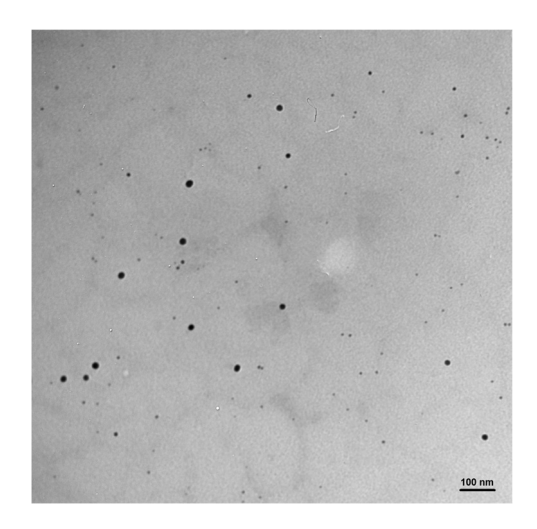


Figure 3: (a) FT-IR spectra of plain AgNO₃, (b) medium molecular weight chitosan (CHI), and (c) AgNPs-CHI.

comparison with those coated with medium molecular weight CHI. This may be attributed to the lower spreadability of the low molecular weight CHI, resulting in an inefficient coating [42,43]. In addition, the low zeta potential resulting from such an inefficient coating might have allowed a higher aggregation tendency of AgNPs due to

Figure 4: Examination of the morphology of the optimized AgNPs-CHI by SEM at (a) low magnification and (b) high magnification. Scale bars represent 1 and 0.5 μ m, respectively.



DE GRUYTER

Figure 5: Examination of the morphology of the optimized AgNPs-CHI by TEM. The scale bar represents 100 nm.

the low repulsive forces, with a subsequent increase in the particle size and particle size polydispersity [44]. Previous reports demonstrated that aggregation of AgNPs has a negative impact on their cytotoxic activity [45,46]. On the other hand, other reports pointed out that the ultrafine nature of some AgNPs formulations may also exert a negative impact on their colloidal stability and biological

performance [47,48]. Considering the earlier considerations, AgNPs with a moderate particle size and a high zeta potential would be favorable from a biological point of view. Therefore, medium molecular weight CHI was selected for further investigations. The optimized AgNPs-CHI demonstrated acceptable size and polydispersity, while the highly-positive zeta potential suggested successful coating of AgNPs with CHI. In addition, UV-Vis spectroscopy confirmed the successful formation of AgNPs, as evidenced by the strong absorption band in the visible region owing to their pronounced surface plasmon resonance effect. AgNPs-CHI spectrum had a maximum absorption wavelength (λ_{max}) of 405 nm, which revealed a successful preparation of AgNPs as well as a spherical morphology of the obtained particles [49]. Furthermore, symmetrical particle size distribution was also predicted from the presence of one absorption band as reported previously [50]. FT-IR spectra confirmed the successful coating of AgNPs with CHI, as suggested by the disappearance of the double-spike peak of the NH2 group of the pure CHI, which indicated a strong interaction between the NH₂ group in CHI and the silver [51]. Examination of the optimized AgNPs-CHI by various electron microscopes, SEM and TEM, confirmed their spherical morphology and colloidal stability. Meanwhile, the size values shown by TEM were mostly corresponding to the metallic silver core, contrary to

Table 2: The physicochemical properties of AgNPs-CHI after a 3-month storage period at different conditions (n = 6, average \pm standard deviation)*

	Hydrodynamic diameter (nm)	PDI	ζ Potential (mV)
Freshly prepared	287.43 ± 1.89	0.411 ± 0.06	50.63 ± 2.2
Stored at 4°C	293.68 ± 2.88	0.405 ± 0.09	52.21 ± 3.1
Stored at room temperature	290.53 ± 3.54	0.428 ± 0.11	49.32 ± 1.7

^{*}The physicochemical properties were evaluated using DLS.

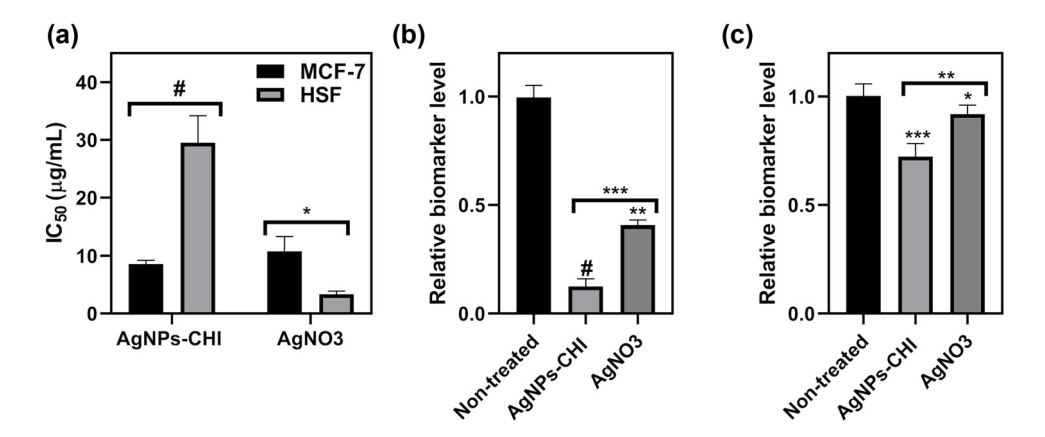


Figure 6: AgNPs-CHI exerts a potent and selective intrinsic anticancer activity against MCF-7 cells. (a) Half-maximal inhibitory concentration (IC₅₀) values of AgNPs-CHI and AgNO₃ solutions evaluated on breast cancer cells (MCF-7) and normal human cells (HSF) 48 h post treatment. *P < 0.05, #P < 0.0001. (b) Relative levels of Interleukin 6 (IL-6) in MCF-7 cells lysates 48 h post treatment with AgNPs-CHI or AgNO₃ solutions at their corresponding IC₅₀ values. **P < 0.01, #P < 0.0001 versus non-treated cells. ***P < 0.001 for AgNPs-CHI versus AgNO₃. (c) Relative levels of TNF-α in MCF-7 cells lysates 48 h post treatment with AgNPs-CHI or AgNO₃ solutions at their corresponding IC₅₀ values. *P < 0.05, ***P < 0.001 versus non-treated cells. **P < 0.01 for AgNPs-CHI versus AgNO₃. In all panels, P = 0.01 results are expressed as mean ± standard deviation.

the DLS measurements that showed the hydrodynamic diameter of the whole nanoparticle [52].

Interestingly, the AgNPs-CHI demonstrated high physical stability upon long-term storage at either room temperature or 4°C. This high stability may be attributed to the high zeta potential imparted by the CHI coating, which minimized interactions between the nanoparticles and inhibited the formation of aggregates [53]. Furthermore, the capability of AgNPs-CHI to retain their stability and physicochemical properties after prolonged storage at room temperature is an amazing advantage that promotes their clinical potential, unlike the vast majority of nanomedicines [13].

The functional coating of AgNPs retained their cytotoxicity to MCF-7 cells, as evidenced by a comparable IC₅₀ value to that of the plain AgNO3. Pure CHI showed minimal cytotoxicity to MCF-7 cells, which excludes its additive cytotoxic effect on the overall cell viability evaluated by the MTT assay in the case of AgNPs-CHI and suggests high tolerability. Surprisingly, the functional coating with CHI resulted in a dramatic improvement in the selectivity of MCF-7 cells in comparison with a normal human cell line, HSF. Although we are still investigating the exact mechanism accounting for such a phenomenon, there are possible reasons that can be considered. First, the increased metabolic activity by cancer cells increases their affinity to carbohydrates and their associated polymers such as CHI, with a subsequent higher cellular uptake of CHI-coated particles by cancer cells compared to normal cells [41]. Second, it has been reported that the polyanionic Heparan Sulfate Proteoglycans (HSPGs) are

upregulated in the cellular membranes of cancer cells, which increases their affinity to positively charged particles like AgNPs-CHI (zeta potential ~50 mV) [54-56]. Third, CHI has an acidic acid dissociation constant (p K_a) ~6.5 which may favor its protonation in the acidic tumorous microenvironment of MCF-7 cells compared to the normal cells, with a subsequent improvement in the cellular uptake [57,58]. Fourth, CHI may modulate the intracellular release of Ag⁺ and the interactions with the subcellular organelles such as mitochondria and nucleus following the cellular uptake, which can be speculated from the improved inhibitory effects on IL-6 and TNF-α in comparison with the plain uncoated AgNO₃ [59,60]. On the other hand, the plain AgNO₃ resulted in non-selective cytotoxicity which was mostly irrelevant to the anticancer activity, as indicated by their inferior impact on IL-6 and TNF-α. Figure 7 outlines the proposed mechanism of the selective cytotoxic effect of AgNPs-CHI against breast cancer cells.

Although some previous studies pointed to the cytotoxic effects of AgNPs against MCF-7 cells, the results shown in the present study were significantly better. A previous analysis by Tao *et al.* revealed that uncoated AgNPs induced cytotoxicity to MCF-7 cells at IC₅₀ of 150 µg/mL [61]. Similarly, in a second study by Sangour *et al.*, the IC₅₀ of the uncoated AgNPs on the same cell line was higher than 100 µg/mL [62]. In a third study by Hepokur and co-workers, uncoated AgNPs did not show a significant cytotoxicity to MCF-7 cells until being loaded with the cytotoxic drug, capecitabine, which then demonstrated an IC₅₀ of 41.25 µg/mL [63]. Upon comparing these

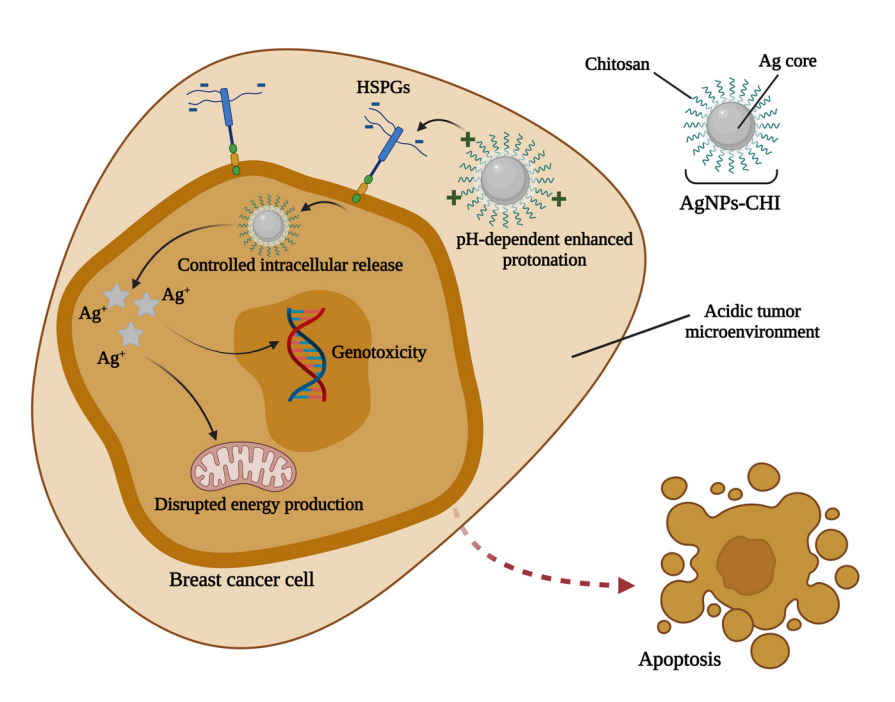


Figure 7: An illustration outlining the proposed mechanism of the selective anticancer activity of AgNPs-CHI against breast cancer cells. The acidic tumor microenvironment promotes the protonation of chitosan, which may improve the interactions of AgNPs-CHI with the polyanionic HSPGs that are overexpressed on the cancer cells. Following the cellular uptake, the chitosan functional coating modulates the intracellular release of silver ions that accumulate into the nucleus resulting in genotoxicity, and in the mitochondria with subsequent disruption of the energy production, which collectively induces cellular apoptosis. Abbreviations: AgNPs-CHI, chitosan-capped silver nanoparticles; HSPGs, heparan sulfate proteoglycans. The figure was created with BioRender.com software, with a publication license (YS24N8UP2Z).

findings with our present results, the value of CHI coating, investigated in the present study, can be speculated. We believe that the amazing finding presented in this study would be promising for future clinical applications, considering the collective advantages of the prepared AgNPs-CHI including the one-pot scalable preparation method, high stability at room temperature, high potency, high selectivity, and high biotolerability. Furthermore, the intrinsic drug-free anticancer activity of AgNPs-CHI is promising to reduce their production cost and extend their industrial applicability as a novel anticancer therapeutic modality.

5 Conclusions

We investigated the impact of the functional coating of AgNPs with CHI on their physicochemical and biological performance on breast cancer cells. Coating AgNPs with medium molecular weight CHI resulted in better physicochemical properties compared to the low molecular weight polymer. Spectroscopical analyses confirmed the successful functional coating of AgNPs. AgNPs-CHI demonstrated a high physical stability for up to 3 months upon storage

either at room temperature or at 4°C. AgNPs-CHI demonstrated a potent and selective anticancer activity on breast cancer cells compared to normal human cells, with a significant inhibitory effect on IL-6 and TNF- α , contrary to the plain AgNO $_3$ which resulted in non-selective cytotoxicity and inferior effects on the relevant tumor markers. The novel, scalable, stable, economic, selective, and drug-free therapeutic modality presented in this study is highly promising for potential clinical applications in the treatment of breast cancer, which would overcome the shortcomings of the existing chemotherapeutics. We are proceeding with its *in vivo* applicability in our upcoming research.

Acknowledgments: The researchers would like to thank the Deanship of Scientific Research, Qassim University, for funding this project. The authors also thank Qassim University for providing technical support.

Funding information: The authors extend their appreciation to the Deputyship for Research and Innovation, Ministry of Education, Saudi Arabia, for funding this research work through project number (QU-IF-1-2-1). The authors also thank the technical support of Qassim University.

Author contributions: Ahmed A. H. Abdellatif: conceptualization, investigation, methodology, data curation, validation, writing-review and editing, and funding acquisition; Ahmed Abdelfattah: methodology, investigation, and data curation. Mahmoud A. Younis: data curation, validation, visualization, and writing the manuscript draft. Saed M. Aldalaan: visualization, methodology, data curation, and validation. Hesham M. Tawfeek: conceptualization, investigation, methodology, supervision, and writing-review and editing. All authors have accepted responsibility for the entire content of this manuscript and approved its submission.

Conflict of interest: The authors state no conflict of interest.

Data availability statement: The datasets generated during and/or analysed during the current study are available from the corresponding author on reasonable request.

References

- Younis MA, Khalil IA, Harashima H. Gene therapy for hepatocellular carcinoma: Highlighting the journey from theory to clinical applications. Adv Ther. 2020;3:2000087.
- [2] Nakamura T, Sato Y, Yamada Y, Abd Elwakil MM, Kimura S, Younis MA, et al. Extrahepatic targeting of lipid nanoparticles in vivo with intracellular targeting for future nanomedicines. Adv Drug Deliv Rev. 2022;188:114417.
- [3] Sung H, Ferlay J, Siegel RL, Laversanne M, Soerjomataram I, Jemal A, et al. Global Cancer Statistics 2020: GLOBOCAN estimates of incidence and mortality worldwide for 36 cancers in 185 countries. CA Cancer J Clin. 2021;71:209–49.
- [4] Ahirwar R. Recent advances in nanomaterials-based electrochemical immunosensors and aptasensors for HER2 assessment in breast cancer. Mikrochim Acta. 2021;188:317.
- [5] Coates AS, Winer EP, Goldhirsch A, Gelber RD, Gnant M, Piccart-Gebhart M, et al. Tailoring therapies-improving the management of early breast cancer: St Gallen International Expert Consensus on the Primary Therapy of Early Breast Cancer 2015. Ann Oncol Off J Eur Soc Med Oncol. 2015:26:1533-46.
- [6] Goldhirsch A, Winer EP, Coates AS, Gelber RD, Piccart-Gebhart M, Thürlimann B, et al. Personalizing the treatment of women with early breast cancer: Highlights of the St Gallen international expert consensus on the primary therapy of early breast cancer 2013. Ann Oncol Off J Eur Soc Med Oncol. 2013;24:2206–23.
- [7] Probst CE, Zrazhevskiy P, Bagalkot V, Gao X. Quantum dots as a platform for nanoparticle drug delivery vehicle design. Adv Drug Deliv Rev. 2013;65:703–18.
- [8] Aleksandrowicz R, Taciak B, Krol M. Drug delivery systems improving chemical and physical properties of anticancer

- drugs currently investigated for treatment of solid tumors.

 J Physiol Pharmacol Off J Pol Physiol Soc. 2017;68:165-74.
- [9] Younis MA, Hetta HF, Abdel-Malek MAY, Ali HRH, Atia NN, Tawfeek HM. Combining acetyl salicylic acid and rofecoxib into novel oral tablets normalize platelet function with potential higher tolerability in patients with cardiovascular disorders. J Drug Deliv Sci Technol. 2020;59:101851.
- [10] Bhanumathi R, Manivannan M, Thangaraj R, Kannan S. Drugcarrying capacity and anticancer effect of the folic acid- and berberine-loaded silver nanomaterial to regulate the AKT-ERK pathway in breast cancer. ACS Omega. 2018;3:8317-28.
- [11] Zhang D, Zhang J. Surface engineering of nanomaterials with phospholipid-polyethylene glycol-derived functional conjugates for molecular imaging and targeted therapy. Biomaterials. 2020;230:119646.
- [12] Abdellatif AAH, Tawfeek HM. Development and evaluation of fluorescent gold nanoparticles. Drug Dev Ind Pharm. 2018;44:1679–84.
- [13] Younis MA, Tawfeek HM, Abdellatif AAH, Abdel-Aleem JA, Harashima H. Clinical translation of nanomedicines: Challenges, opportunities, and keys. Adv Drug Deliv Rev. 2022;181:114083.
- [14] Abdellatif AAH, Younis MA, Alsharidah M, Al Rugaie O, Tawfeek HM. Biomedical applications of quantum dots: Overview, challenges, and clinical potential. Int J Nanomed. 2022;17:1951-70.
- [15] Jeong J-K, Gurunathan S, Kang M-H, Han JW, Das J, Choi Y-J, et al. Hypoxia-mediated autophagic flux inhibits silver nanoparticle-triggered apoptosis in human lung cancer cells. Sci Rep. 2016;6:21688.
- [16] Heydari R. Biological applications of biosynthesized silver nanoparticles through the utilization of plant extracts. Herb Med J. 2017;2:87–95.
- [17] Kovács D, Igaz N, Gopisetty MK, Kiricsi M. Cancer therapy by silver nanoparticles: Fiction or reality? Int J Mol Sci. 2022:23:839.
- [18] Tang Y, Liang J, Wu A, Chen Y, Zhao P, Lin T, et al. Co-delivery of trichosanthin and albendazole by nano-self-assembly for overcoming tumor multidrug-resistance and metastasis. ACS Appl Mater Interfaces. 2017;9:26648-64.
- [19] Huy TQ, Huyen PTM, Le AT, Tonezzer M. Recent advances of silver nanoparticles in cancer diagnosis and treatment. Anti-Cancer Agents Med Chem. 2020;20:1276–87.
- [20] Shanmugasundaram T, Radhakrishnan M, Gopikrishnan V, Kadirvelu K, Balagurunathan R. Biocompatible silver, gold and silver/gold alloy nanoparticles for enhanced cancer therapy: in vitro and in vivo perspectives. Nanoscale. 2017;9:16773–90.
- [21] Mohamed N. Synthesis of hybrid chitosan silver nanoparticles loaded with doxorubicin with promising anti-cancer activity. BioNanoScience. 2020;10:758-65.
- [22] Heydari R, Rashidipour M. Green synthesis of silver nanoparticles using extract of oak fruit hull (jaft): Synthesis and in vitro cytotoxic effect on mcf-7 cells. Int J Breast Cancer. 2015;2015:846743.
- [23] Rashidipour M, Heydari R. Biosynthesis of silver nanoparticles using extract of olive leaf: synthesis and in vitro cytotoxic effect on MCF-7 cells. J Nanostruct Chem. 2014;4:112.
- [24] Cotton GC, Gee C, Jude A, Duncan WJ, Abdelmoneim D, Coates DE. Efficacy and safety of alpha lipoic acid-capped

silver nanoparticles for oral applications. RSC Adv. 2019:9:6973-85.

DE GRUYTER

- [25] Verma SK, Jha E, Panda PK, Mishra A, Thirumurugan A, Das B, et al. Rapid novel facile biosynthesized silver nanoparticles from bacterial release induce biogenicity and concentration dependent in vivo cytotoxicity with embryonic zebrafish-a mechanistic insight. Toxicol Sci Off J Soc Toxicol. 2018:161:125-38.
- [26] Pinzaru I, Coricovac D, Dehelean C, Moacă EA, Mioc M, Baderca F, et al. Stable PEG-coated silver nanoparticles - A comprehensive toxicological profile. Food Chem Toxicol Int J Publ Br Ind Biol Res Assoc. 2018;111:546-56.
- [27] Abdellatif AAH, Alsharidah M, Al Rugaie O, Tawfeek HM, Tolba NS. Silver nanoparticle-coated ethyl cellulose inhibits tumor necrosis factor-α of breast cancer cells. Drug Des Dev Ther. 2021:15:2035-46.
- [28] Jiménez-Gómez CP, Cecilia JA. Chitosan: A natural biopolymer with a wide and varied range of applications. Molecules. 2020:25:3981.
- [29] Javed R, Zia M, Naz S, Aisida SO, Ain Nu, Ao Q. Role of capping agents in the application of nanoparticles in biomedicine and environmental remediation: recent trends and future prospects. J Nanobiotechnol. 2020;18:172.
- [30] Franconetti A, Carnerero JM, Prado-Gotor R, Cabrera-Escribano F, Jaime C. Chitosan as a capping agent: Insights on the stabilization of gold nanoparticles. Carbohydr Polym. 2019;207:806-14.
- [31] Mi F-L, Wu S-J, Zhong W-Q, Huang C-Y. Preparation of a silver nanoparticle-based dual-functional sensor using a complexation-reduction method. Phys Chem Chem Phys. 2015;17:21243-53.
- [32] Younis MA, Sato Y, Elewa YHA, Kon Y, Harashima H. Selfhoming nanocarriers for mRNA delivery to the activated hepatic stellate cells in liver fibrosis. J Control Release Off J Control Rel Soc. 2023;353:685-98.
- [33] Atia NN, Tawfeek HM, Rageh AH, El-Zahry MR, Abdelfattah A, Younis MA. Novel sublingual tablets of Atorvastatin calcium/ Trimetazidine hydrochloride combination; HPTLC quantification, in vitro formulation and characterization. Saudi Pharm J SPI Off Publ Saudi Pharm Soc. 2019:27:540-9.
- [34] Aboutaleb AE, Abdel-rahman SI, Ahmed MO, Younis MA. Design and evaluation of domperidone sublingual tablets. Int J Pharm Pharm Sci. 2016;8:195-201.
- [35] Younis MA, El-Zahry MR, Tallat MA, Tawfeek HM. Sulpiride gastro-retentive floating microsponges; analytical study, in vitro optimization and in vivo characterization. J Drug Target. 2020;28:386-97.
- [36] Tawfeek HM, Abdellatif AAH, Abdel-Aleem JA, Hassan YA, Fathalla D. Transfersomal gel nanocarriers for enhancement the permeation of lornoxicam. J Drug Deliv Sci Technol. 2020;56:101540.
- [37] Younis MA, Khalil IA, Abd Elwakil MM, Harashima H. A multifunctional lipid-based nanodevice for the highly specific codelivery of sorafenib and midkine siRNA to hepatic cancer cells. Mol Pharm. 2019;16:4031-44.
- [38] Younis MA, Khalil IA, Elewa YHA, Kon Y, Harashima H. Ultrasmall lipid nanoparticles encapsulating sorafenib and midkine-siRNA selectively-eradicate sorafenib-resistant hepatocellular carcinoma in vivo. Off J Control Rel Soc. 2021;331:335-49.

- [39] Gomes HIO, Martins CSM, Prior JAV. Silver nanoparticles as carriers of anticancer drugs for efficient target treatment of cancer cells. Nanomaterials (Basel). 2021;11:964.
- [40] Gomathi AC, Xavier Rajarathinam SR, Mohammed Sadiq A, Rajeshkumar S. Anticancer activity of silver nanoparticles synthesized using aqueous fruit shell extract of Tamarindus indica on MCF-7 human breast cancer cell line. J Drug Deliv Sci Technol. 2020:55:101376.
- [41] Buttacavoli M, Albanese NN, Di Cara G, Alduina R, Faleri C, Gallo M, et al. Anticancer activity of biogenerated silver nanoparticles: an integrated proteomic investigation. Oncotarget. 2017;9:9685-705.
- [42] Kouchak M, Avadi M, Abbaspour M, Jahangiri A, Boldaji SK. Effect of different molecular weights of chitosan on preparation and characterization of insulin loaded nanoparticles by ion gelation method. Int J Drug Dev Res. 2012;4:271-7.
- [43] Kapadnis G, Dey A, Dandekar P, Jain R. Effect of degree of deacetylation on solubility of low-molecular-weight chitosan produced via enzymatic breakdown of chitosan. Polym Int. 2019;68:1054-63.
- [44] Bathi JR, Roy S, Tareq S, Potts GE, Palchoudhury S, Sweck SO, et al. Dispersion and aggregation fate of individual and coexisting metal nanoparticles under environmental aqueous suspension conditions. Mater (Basel, Switz). 2022;15:6733.
- Bélteky P, Rónavári A, Igaz N, Szerencsés B, Tóth IY, Pfeiffer I, et al. Silver nanoparticles: aggregation behavior in biorelevant conditions and its impact on biological activity. Int J Nanomed. 2019;14:667-87.
- [46] Kong IC, Ko KS, Koh DC. Evaluation of the Effects of Particle Sizes of Silver Nanoparticles on Various Biological Systems. Int J Mol Sci. 2020;21:8465.
- [47] Fehaid A, Taniguchi A. The double-edged effect of silver nanoparticles is determined by their physical characteristics. Nano Biomed. 2019;11:49-56.
- [48] Bélteky P, Rónavári A, Zakupszky D, Boka E, Igaz N, Szerencsés B, et al. Are smaller nanoparticles always better? Understanding the biological effect of size-dependent silver nanoparticle aggregation under biorelevant conditions. Int J Nanomed. 2021;16:3021-40.
- [49] Roe D, Karandikar B, Bonn-Savage N, Gibbins B, Roullet JB. Antimicrobial surface functionalization of plastic catheters by silver nanoparticles. J Antimicrob Chemother. 2008;61:869-76.
- [50] Hajji S, Salem RBS-B, Hamdi M, Jellouli K, Ayadi W, Nasri M, et al. Nanocomposite films based on chitosan-poly(vinyl alcohol) and silver nanoparticles with high antibacterial and antioxidant activities. Process Saf Environ Prot. 2017:111:112-21.
- [51] Nate Z, Moloto MJ, Mubiayi PK, Sibiya PN. Green synthesis of chitosan capped silver nanoparticles and their antimicrobial activity. MRS Adv. 2018;3:2505-17.
- [52] Fissan H, Ristig S, Kaminski H, Asbach C, Epple M. Comparison of different characterization methods for nanoparticle dispersions before and after aerosolization. Anal Methods. 2014;6:7324-34.
- [53] Kaufman ED, Belyea J, Johnson MC, Nicholson ZM, Ricks JL, Shah PK, et al. Probing protein adsorption onto mercaptoundecanoic acid stabilized gold nanoparticles and surfaces by quartz crystal microbalance and zeta-potential measurements. Langmuir ACS J Surf Colloids. 2007;23:6053-62.

- [54] Nagarajan A, Malvi P, Wajapeyee N. Heparan sulfate and heparan sulfate proteoglycans in cancer initiation and progression. Front Endocrinol (Lausanne). 2018;9:483-3.
- [55] Hatabe S, Kimura H, Arao T, Kato H, Hayashi H, Nagai T, et al. Overexpression of heparan sulfate 6-O-sulfotransferase-2 in colorectal cancer. Mol Clin Oncol. 2013:1:845–50.
- [56] De Pasquale V, Pavone LM. Heparan sulfate proteoglycan signaling in tumor microenvironment. Int J Mol Sci. 2020;21:6588.
- [57] Mohammed MA, Syeda JTM, Wasan KM, Wasan EK. An overview of chitosan nanoparticles and its application in non-parenteral drug delivery. Pharmaceutics. 2017;9:53.
- [58] Montcourrier P, Silver I, Farnoud R, Bird I, Rochefort H. Breast cancer cells have a high capacity to acidify extracellular milieu by a dual mechanism. Clin Exp Metastasis. 1997;15:382–92.

- [59] Biba R, Košpić K, Komazec B, Markulin D, Cvjetko P, Pavoković D, et al. Surface coating-modulated phytotoxic responses of silver nanoparticles in plants and freshwater green algae. Nanomaterials (Basel). 2021;12:24.
- [60] Jin S, Li J, Wang J, Jiang J, Zuo Y, Li Y, et al. Electrospun silver ion-loaded calcium phosphate/chitosan antibacterial composite fibrous membranes for guided bone regeneration. Int J Nanomed. 2018:13:4591–605.
- [61] Tao L, Chen X, Sun J, Wu C. Silver nanoparticles achieve cytotoxicity against breast cancer by regulating long-chain noncoding RNA XLOC_006390-mediated pathway. Toxicol Res. 2021;10:123-33.
- [62] Sangour MH, Ali IM, Atwan ZW, Al Ali AAALA. Effect of Ag nanoparticles on viability of MCF-7 and Vero cell lines and gene expression of apoptotic genesEgyptian. J Med Hum Genet. 2021;22:9.
- [63] Hepokur C, Kariper İA, Mısır S, Ay E, Tunoğlu S, Ersez MS, et al. Silver nanoparticle/capecitabine for breast cancer cell treatment. Toxicol Vitro. 2019;61:104600.